

Towards a Co-Design Framework for Future Mobility Systems

Gioele Zardini (Corresponding Author)

Stanford University, Aeronautics and Astronautics
496 Lomita Mall, Stanford, CA 94305-4035, USA
E-mail: gzardini@ethz.ch

Nicolas Lanzetti

Stanford University, Aeronautics and Astronautics
496 Lomita Mall, Stanford, CA 94305-4035, USA
E-mail: lnicolas@ethz.ch

Mauro Salazar, Ph.D.

Stanford University, Aeronautics and Astronautics
496 Lomita Mall, Stanford, CA 94305-4035, USA
E-mail: samauro@stanford.edu

Andrea Censi, Ph.D.

ETH Zurich, Institute for Dynamic Systems and Control
Sonneggstrasse 3, 8092 Zurich, ZH-Switzerland
E-mail: acensi@ethz.ch

Emilio Frazzoli, Ph.D.

ETH Zurich, Institute for Dynamic Systems and Control
Sonneggstrasse 3, 8092 Zurich, ZH-Switzerland
E-mail: emilio.frazzoli@idsc.mavt.ethz.ch

Marco Pavone, Ph.D.

Stanford University, Aeronautics and Astronautics
496 Lomita Mall, Stanford, CA 94305-4035, USA
E-mail: pavone@stanford.edu

Word Count: 7241 words + 1 table(s) \times 250 = 7491 words

Submission Date: October 14, 2019

1. Abstract

The design of Autonomous Vehicles (AVs) and the design of AVs-enabled mobility systems are closely coupled. Indeed, knowledge about the intended service of AVs would impact their design and deployment process, whilst insights about their technological development could significantly affect transportation management decisions. This calls for tools to study such a coupling and co-design AVs and AVs-enabled mobility systems in terms of different objectives. In this paper, we instantiate a framework to address such co-design problems. In particular, we leverage the recently developed theory of co-design to frame and solve the problem of designing and deploying an intermodal Autonomous Mobility-on-Demand system, whereby AVs service travel demands jointly with public transit, in terms of fleet sizing, vehicle autonomy, and public transit service frequency. Our framework is modular and compositional, allowing to describe the design problem as the interconnection of its individual components and to tackle it from a system-level perspective. Moreover, it only requires very general monotonicity assumptions and it naturally handles multiple objectives, delivering the *rational* solutions on the Pareto front and thus enabling policy makers to select a solution through “political” criteria. To showcase our methodology, we present a real-world case study for Washington D.C., USA. Our work suggests that it is possible to create user-friendly optimization tools to systematically assess the costs and benefits of interventions, and that such analytical techniques might gain a momentous role in policy-making in the future.

Keywords: Co-Design, Autonomous Vehicles, Future Mobility Systems.

2. Introduction

Arguably, the current design process for Autonomous Vehicles (AVs) largely suffers from the lack of clear, specific requirements in terms of the service such vehicles will be providing. Yet, knowledge about their intended service (e.g., last-mile versus point-to-point travel) might dramatically impact how the AVs are designed, and, critically, significantly ease their development process. For example, if for a given city we knew that for an effective on-demand mobility system autonomous cars only need to drive up to 25 mph and only on relatively easy roads, their design would be greatly simplified and their deployment could certainly be accelerated. At the same time, from the system-level perspective of transportation management, knowledge about the trajectory of technology development for AVs would certainly impact decisions on infrastructure investments and provision of service. In other words, the design of the AVs and the design of a mobility system leveraging AVs are intimately *coupled*. This calls for methods to reason about such a coupling, and in particular to *co-design* the AVs and the associated AVs-enabled mobility system. A key requirement in this context is to be able to account for a range of heterogeneous objectives that are often not directly comparable (consider, for instance, travel time and emissions).

Accordingly, the goal of this paper is to lay the foundations for a framework through which one can co-design future AVs-enabled mobility systems. Specifically, we show how one can leverage the recently developed mathematical theory of co-design [1–3], which provides a general methodology to co-design complex systems in a modular and compositional fashion. This tool delivers the set of rational design solutions lying on the Pareto front, allowing to reason about the costs and benefits of the individual design options. The framework is instantiated in the setting of co-designing intermodal Autonomous Mobility-on-Demand (AMoD) systems [4], whereby fleets of self-driving vehicles provide on-demand mobility jointly with public transit. Aspects that are subject to co-design include fleet size, vehicle-specific characteristics for the AVs, and public transit service frequency.

Literature Review: The design of mobility systems can be divided in classic urban transportation network design problems and more recent design problems for AMoD systems. The first research stream was reviewed in [5] and can be divided in road [6, 7], public transit [8, 9], and multi-modal [10] network design problems which can be classified as *strategic* long-term infrastructure modification decisions such as building new streets, *tactical* infrastructure-allocation problems on lanes allocation and public transit service frequency, and *operational* short-term scheduling problems. They are usually formulated as bilevel problems whereby the upper-level is related to the policy in discussion and the lower-level is concerned with solving the trip assignment problem by computing the user equilibrium or the system optimum under given congestion and demand models. Overall, these problems are solved with non-convex and combinatorial mathematical methods, heuristics, and metaheuristics consisting of gradient-free optimization algorithms. Often, the problems are formulated with a unique objective or, in the case of multi-objective settings, the different objectives are reduced to a unique one through monetary metrics precluding Pareto solutions. The design of AMoD systems mostly considers their fleet sizing. In particular, it was studied through simulations in [11–13] and with analytical methods in [14], whilst in [15] the problem was combined with the charging infrastructure sizing and placement problem and solved using mixed integer linear programming techniques. The fleet sizing and vehicle allocation problem for conventional vehicles was presented in [16]. The fleet size and pricing scheme of Mobility-on-Demand systems was designed in [17] with Bayesian optimization, whereas in [18] a rail-car fleet sizing problem was solved with simulated annealing. More recently, the joint design of multimodal

transit networks and AMoD systems was formulated in [19] as a bilevel optimization problem and solved with heuristic methods. Overall, to the best of the authors' knowledge, most design methods for AMoD rely either on simulation-based approaches or nonlinear and combinatorial optimization techniques, and do not study AVs-specific characteristics such as the achievable vehicle speed. In conclusion, the frameworks proposed for the design of mobility systems mainly have a fixed problem-specific structure and are thus non-modular. Moreover, they do not deliver a Pareto front of solutions, focusing on a unique objective.

Statement of Contribution: In this paper we lay the foundations for the systematic study of the design of AVs-enabled mobility systems. Specifically, we leverage the mathematical theory of co-design [1] to devise a framework to study the design of intermodal AMoD (I-AMoD) systems in terms of fleet characteristics and public transit service, enabling the computation of the *rational* solutions lying on the Pareto front of minimal travel time, transportation costs, and emissions. Our framework allows to structure the design problem in a modular way, in which each different transportation option can be “plugged in” in a larger model. Each model has minimal assumptions: Rather than properties such as linearity and convexity, we ask for very general monotonicity assumptions. For example, we assume that the cost of automation increases monotonically with the speed achievable by the self-driving car. We are able to obtain the full Pareto front of *rational* solutions, or, given more “political” criteria, to weigh incomparable costs (such as travel time and emissions), to present one optimal solution to stakeholders, such as AVs companies and municipalities. We consider the real-world case study for Washington D.C., to showcase our methodology. We show how, given the model, we can easily formulate and answer several questions regarding the introduction of new technologies and investigate possible infrastructure interventions.

2.1. Organization

The remainder of this paper is structured as follows: Section 3 presents the mathematical background of co-design. Section 4 presents the co-design problem for AVs-enabled mobility systems. We showcase our approach with real-world case studies for Washington D.C., USA, in Section 5. Section 6 concludes the paper with a discussion and an overview on future research directions.

3. Mathematical Background

In this section, we present the basics of partial order theory and the mathematical theory of co-design. The interested reader is referred to [1–3].

Partial Order Theory

Consider a set \mathcal{P} and a partial order $\preceq_{\mathcal{P}}$, defined as a reflexive, antisymmetric, and transitive relation [20]. Then, \mathcal{P} and $\preceq_{\mathcal{P}}$ define the partially ordered set (poset) $\langle \mathcal{P}, \preceq_{\mathcal{P}} \rangle$. The least and maximum elements of a poset are called bottom and top, and are denoted by $\perp_{\mathcal{P}}$ and $\top_{\mathcal{P}}$, respectively. A set $S \subseteq \mathcal{P}$ is *directed* if each pair of elements $x, y \in S$ has an upper bound. A poset is a *directed complete partial order* (DCPO) if each of its directed subsets has a top, and it is a *complete partial order* (CPO) if it has a bottom as well. A *chain* is a subset $S \subseteq \mathcal{P}$ where all elements are comparable, i.e., for $x, y \in S$, $x \preceq_{\mathcal{P}} y$ or $y \preceq_{\mathcal{P}} x$. Conversely, an *antichain* is a subset $S \subseteq \mathcal{P}$ where no elements are comparable, i.e., for $x, y \in S$, $x \preceq_{\mathcal{P}} y$ implies $x = y$. A map $g : \mathcal{P} \rightarrow \mathcal{Q}$ between two posets is *monotone* iff $x \preceq_{\mathcal{P}} y$ implies $g(x) \preceq_{\mathcal{Q}} g(y)$.

Mathematical Theory of Co-Design

As in [1], we abstract a Design Problem (DP) as a monotone map h between provided *function-*

alities and the antichain of required *resources*, represented as elements of the CPOs $\langle \mathcal{F}, \preceq_{\mathcal{F}} \rangle$, $\langle \mathcal{R}, \preceq_{\mathcal{R}} \rangle$, respectively. Different to classical approaches, mostly relying on properties such as continuity, linearity, or convexity, our approach only requires monotone relations between the antichain of resources and the functionalities. The Co-Design Problem (CDP) of the full system results then from the interconnection, typically given in form of a graph, of the DP of its individual components. Indeed, this allows to describe complex models in a modular and compositional fashion. We focus on the problem of finding the antichain of all *rational* resources $r_1, \dots, r_N \in \mathcal{R}$ which provide a given functionality $f \in \mathcal{F}$. Nevertheless, the framework can readily accommodate alternative problem formulations, such as finding the antichain of all rational functionalities $f_1, \dots, f_N \in \mathcal{F}$ which are provided given a resource $r \in \mathcal{R}$. Rather than computing a single solution, this method provides therefore an antichain, or equivalently, a set of incomparable rational decisions.

4. Co-Design of AV-enabled Mobility Systems

In this section, we instantiate our proposed co-design framework in the setting whereby a central, social welfare maximizing authority (e.g., a central authority) strives to co-design a mobility system comprising AMoD and public transportation, in terms of AV fleet size, vehicle-specific characteristics, and public transit service frequency. This rather idealized setting serves a number of purposes: First, it grounds our co-design framework within a concrete urban transportation design problem. Second, the insights we derive can be interpreted as upper bounds on the performance gains one might achieve via co-design. Third, this setting subsumes as special cases the co-design of AV and AMoD services (of interest, e.g., to AV and mobility-as-a-service companies alike) and the co-design of AMoD and intermodal transportation systems (of interest, e.g., to municipal authorities). Fourth, it provides a starting point to address the more challenging (and more realistic) setting whereby multiple stakeholders, with different objectives, might converge via co-design to an optimized transportation system.

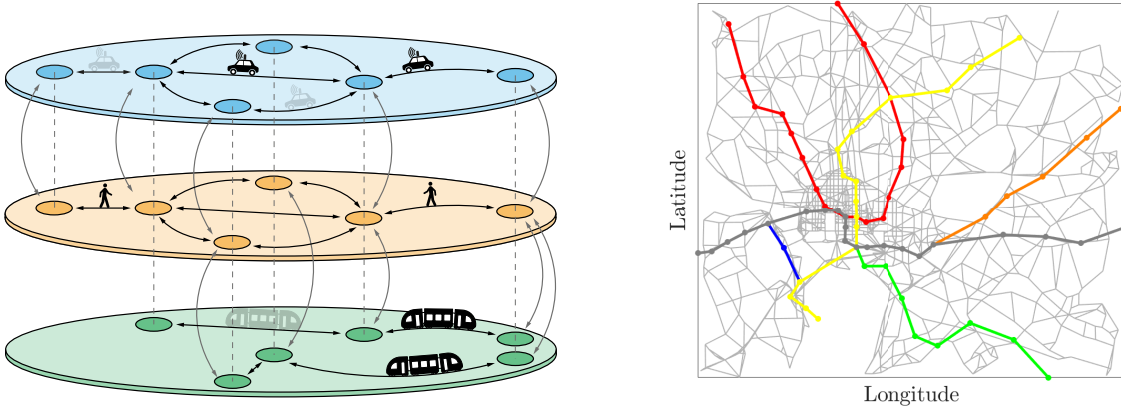
We start by describing in Section 4.1 the urban transportation design problem we want to address in this paper; we then present its associated co-design framework in Section 4.2.

4.1. Intermodal AMoD Framework

In this section, we present the I-AMoD framework from [4] used to describe our setting. We adopt a mesoscopic planning perspective and formulate the problem as a multi-commodity network flow problem, whereby we allow customers to be routed in an intermodal fashion.

4.1.1. Multi-Commodity Flow Model

The transportation system and its different modes are modeled using the digraph $\mathcal{G} = (\mathcal{V}, \mathcal{A})$, shown in Figure 1a. It is composed of a set of nodes \mathcal{V} and a set of arcs $\mathcal{A} \subseteq \mathcal{V} \times \mathcal{V}$. Specifically, it contains a road network layer $\mathcal{G}_R = (\mathcal{V}_R, \mathcal{A}_R)$, a public transportation layer $\mathcal{G}_P = (\mathcal{V}_P, \mathcal{A}_P)$, and a walking layer $\mathcal{G}_W = (\mathcal{V}_W, \mathcal{A}_W)$. The road network is characterized through intersections $i \in \mathcal{V}_R$ and road segments $(i, j) \in \mathcal{A}_R$. Similarly, public transportation lines are modeled through station nodes $i \in \mathcal{V}_P$ and line segments $(i, j) \in \mathcal{A}_P$. The walking network contains walkable streets $(i, j) \in \mathcal{A}_W$ connecting intersections $i \in \mathcal{V}_W$. Our model allows mode-switching arcs $\mathcal{A}_C \subseteq \mathcal{V}_R \times \mathcal{V}_W \cup \mathcal{V}_W \times \mathcal{V}_R \cup \mathcal{V}_P \times \mathcal{V}_W \cup \mathcal{V}_W \times \mathcal{V}_P$ connecting the road and the public transportation layers to the pedestrian layer. Consequently, $\mathcal{V} = \mathcal{V}_W \cup \mathcal{V}_R \cup \mathcal{V}_P$ and $\mathcal{A} = \mathcal{A}_W \cup \mathcal{A}_R \cup \mathcal{A}_P \cup \mathcal{A}_C$. Consistently with the structural properties of road and walking networks in urban environments, we assume the graph \mathcal{G}



(a) Intermodal AMoD network.

(b) Washington D.C. road and subway graphs.

FIGURE 1: (a) The intermodal AMoD network consists of a road, a walking, and a public transportation digraph. The coloured circles represent stops or intersections and the black arrows denote road links, pedestrian pathways, or public transit arcs. The dotted lines represent nodes which are close geographically, while the grey arrows represent the mode-switching arcs connecting them. (b) The Washington D.C. transportation network, consisting of the MetroRail subway lines and the city roads.

to be strongly connected. We model a travel request ρ as a triple $(o, d, \alpha) \in \mathcal{V} \times \mathcal{V} \times \mathbb{R}_+$, described by its origin node o , its destination node d , and its request rate $\alpha > 0$, namely, how many customers want to travel from o to d per unit time. We assume that the origin and destination vertices of the M requests lie in the walking digraph, i.e., $o_m, d_m \in \mathcal{V}_W$ for all $m \in \mathcal{M} := \{1, \dots, M\}$.

The flow $f_m(i, j)$ represents the number of customers per unit time traversing arc $(i, j) \in \mathcal{A}$ and satisfying a travel request m . Furthermore, $f_0(i, j)$ denotes the flow of empty vehicles on road arcs $(i, j) \in \mathcal{A}_R$, accounting for rebalancing flows of AMoD vehicles between a customer's drop-off and the next customer's pick-up. Assuming the vehicles to carry one customer at a time, the flows satisfy

$$\sum_{i:(i,j) \in \mathcal{A}} f_m(i, j) + \mathbb{1}_{j=o_m} \cdot \alpha_m = \sum_{k:(j,k) \in \mathcal{A}} f_m(j, k) + \mathbb{1}_{j=d_m} \cdot \alpha_m, \quad \forall m \in \mathcal{M}, j \in \mathcal{V} \quad (1a)$$

$$\sum_{i:(i,j) \in \mathcal{A}_R} \left(f_0(i, j) + \sum_{m \in \mathcal{M}} f_m(i, j) \right) = \sum_{k:(j,k) \in \mathcal{A}_R} \left(f_0(j, k) + \sum_{m \in \mathcal{M}} f_m(j, k) \right), \quad \forall j \in \mathcal{V}_R \quad (1b)$$

$$f_m(i, j) \geq 0, \quad \forall m \in \mathcal{M}, (i, j) \in \mathcal{A} \quad (1c)$$

$$f_0(i, j) \geq 0, \quad \forall (i, j) \in \mathcal{A}_R, \quad (1d)$$

where $\mathbb{1}_{j=x}$ denotes the boolean indicator function. Specifically, (1a) guarantees flows conservation for every transportation demand, and (1b) preserves flow conservation for vehicles on every road node. Combining conservation of customers (1a) with the conservation of vehicles (1b) guarantees rebalancing vehicles to match the demand. Finally, (1c), (1d) ensure non-negativity of flows.

4.1.2. Travel Time and Travel Speed

The variable t_{ij} denotes the time needed to traverse an arc (i, j) of length s_{ij} . We assume a constant walking speed on pedestrian arcs and infer travel times on public transportation arcs from the public transit schedules. Considering that the public transportation system at node j operates with the frequency ϕ_j , switching from a pedestrian vertex i to a public transit station j takes, on average, $t_{WS} + 1/\phi_j$, where t_{WS} is a constant sidewalk-to-station travel time. We assume that the average waiting time for AMoD vehicles is t_{WR} and that switching from the road graph and the public transit graph to the pedestrian graph takes the transfer times t_{RW} and t_{SW} , respectively. While each road arc $(i, j) \in \mathcal{A}_R$ is characterized by a speed limit $v_{L,ij}$, AVs safety protocols impose a maximum achievable velocity v_a . In order to prevent too slow and therefore dangerous driving behaviours [21], we only consider road arcs through which the AVs can drive at least at a fraction β of the speed limit: Arc $(i, j) \in \mathcal{A}_R$ is kept in the road network if and only if

$$v_a \geq \beta \cdot v_{L,ij}, \quad (2)$$

where $\beta \in (0, 1]$. We set the velocity of all arcs fulfilling condition (2) to $v_{ij} = \min\{v_a, v_{L,ij}\}$ and compute the travel time to traverse them as

$$t_{ij} = \frac{s_{ij}}{v_{ij}}. \quad (3)$$

4.1.3. Road Congestion

In our setting, we assume that each road arc $(i, j) \in \mathcal{A}_R$ is subject to a baseline usage u_{ij} , capturing the presence of exogenous traffic (e.g., private vehicles), and that it has a nominal capacity c_{ij} . Furthermore, we assume that the central authority operates the AMoD fleet such that vehicles travel at free-flow speed throughout the road network of the city, meaning that the total flow on each road link must be below the link's capacity. Therefore, we capture congestion effects with the threshold model

$$f_0(i, j) + \sum_{m \in \mathcal{M}} f_m(i, j) + u_{ij} \leq c_{ij} \quad \forall (i, j) \in \mathcal{A}_R. \quad (4)$$

4.1.4. Energy Consumption

We compute the energy consumption of the AVs for each road link considering an urban driving cycle, scaled so that the average speed $v_{\text{avg,cycle}}$ matches the free-flow speed on the link s_{ij}/t_{ij} , and scale the energy consumption with the length of the arc s_{ij} as

$$e_{ij} = e_{\text{cycle}} \cdot \frac{s_{ij}}{s_{\text{cycle}}} \quad \forall (i, j) \in \mathcal{A}_R. \quad (5)$$

For the public transportation system, we assume a constant energy consumption per unit time. This approximation is acceptable in urban environments, as the operation of the public transportation system is independent from the number of customers serviced, and its energy consumption is therefore customers-invariant.

4.1.5. Fleet Size

We consider a fleet of $n_{v,\max}$ AVs. In a time-invariant setting, the number of vehicles on arc (i, j) is expressed as the multiplication of the total vehicles flow on the arc and its travel time. Therefore,

we constrain the number of vehicles employed as

$$n_{v,e} = \sum_{(i,j) \in \mathcal{A}_R} \left(f_0(i,j) + \sum_{m \in \mathcal{M}} f_m(i,j) \right) \cdot t_{ij} \leq n_{v,\max}. \quad (6)$$

4.1.6. Discussion

A few comments are in order. First, we assume the demand to be time-invariant and allow flows to have fractional values. This assumption is in line with the *mesoscopic* and system-level *planning* perspective of our study. Second, we model congestion using a threshold model. This approach can be interpreted as the municipal authority not allowing the AMoD vehicles to exceed the critical density of the flows on road arcs, so that cars can be assumed to travel at free flow speed [22]. This way, we can assume that the route planning of AMoD vehicles does not influence the exogenous traffic. Finally, in line with the status quo, we allow AMoD vehicles to transport one customer at the time [23]. For further discussions on our modeling assumptions, we refer the readers to [4, 24].

4.2. Co-Design Framework

We integrate the I-AMoD framework presented in Section 4.1 in the co-design formalism, allowing the decoupling of the CDP of a complex system in the DP of its individual components in a modular, compositional, and systematic fashion. We aim to compute the antichain of resources, quantified in terms of costs, average travel time per trip, and emissions required to provide the mobility service to a set of customers. In order to achieve this, we decouple the CDP in the DPs of the individual AV (Section 4.2.1) and of the AVs fleet (Section 4.2.3) as well as of the public transportation system (Section 4.2.2). Their interconnection is presented in Section 4.2.4.

4.2.1. The Autonomous Vehicle Design Problem

The AV DP (Figure 2a) consists of selecting the maximal speed of the AVs. Under the rationale that driving safely at higher speed requires more advanced sensing and algorithmic capabilities, we model the achievable speed of the AVs v_a as a monotone function of the vehicle fixed costs $C_{v,f}$ (resulting from the cost of the vehicle $C_{v,v}$ and the cost of its automation $C_{v,a}$) and the mileage-dependent operational costs $C_{v,o}$ (accounting for maintenance, cleaning, energy consumption, depreciation, and opportunity costs [25]). In this setting, the AV DP provides the functionality v_a and requires the resources $C_{v,f}$ and $C_{v,o}$. Consequently, the functionality space is $\mathcal{F}_v = \overline{\mathbb{R}}_+$ (in mph), and the resources space is $\mathcal{R}_v = \overline{\mathbb{R}}_+ \times \overline{\mathbb{R}}_+$ (in USD \times USD/mile).

4.2.2. The Subway Design Problem

We design the public transit infrastructure (Figure 2b) by means of the service frequency introduced in Section 4.1.2. Specifically, we assume the service frequency φ_j to scale linearly with the size of the train fleet n_s as

$$\frac{\varphi_j}{\varphi_{j,\text{baseline}}} = \frac{n_s}{n_{s,\text{baseline}}}. \quad (7)$$

We relate a train fleet of size n_s to the fixed costs $C_{s,f}$ (accounting for train and infrastructural costs) and to the operational costs $C_{s,o}$ (accounting for energy consumption, vehicles depreciation, and train operators' wages). Given the passengers-independent public transit operation in today's cities, we reasonably assume the operational costs $C_{s,o}$ to be mileage independent and to only

vary with the size of the fleet. Formally, the number of acquired trains $n_{s,a} = n_s - n_{s,\text{baseline}}$ is a functionality, whereas $C_{s,f}$ and $C_{s,o}$ are resources. The functionality space is $\mathcal{F}_s = \mathbb{N}$ and the resources space is $\mathcal{R}_s = \overline{\mathbb{R}}_+ \times \overline{\mathbb{R}}_+$ (in $\text{USD} \times \text{USD}/\text{year}$).

4.2.3. The I-AMoD Optimization Framework Design Problem

The I-AMoD DP (see Figure 2c) provides the demand satisfaction as a functionality, expressed through the total customer request rate

$$\alpha_{\text{tot}} := \sum_{m \in \mathcal{M}} \alpha_m. \quad (8)$$

To successfully satisfy a given set of travel requests, we require the following resources: (i) the achievable speed of the AVs v_a , (ii) the number of available AVs per fleet $n_{v,\text{max}}$, (iii) the number of trains $n_{s,a}$ acquired by the public transportation system, and (iv) the average travel time of a trip

$$t_{\text{avg}} := \frac{1}{\alpha_{\text{tot}}} \cdot \sum_{m \in \mathcal{M}, (i,j) \in \mathcal{A}} t_{ij} \cdot f_m(i, j), \quad (9)$$

(v) the total distance driven by the AVs per unit time

$$s_{v,\text{tot}} := \sum_{(i,j) \in \mathcal{A}_R} s_{ij} \cdot \left(f_0(i, j) + \sum_{m \in \mathcal{M}} f_m(i, j) \right), \quad (10)$$

and (vi) the total AVs CO₂ emissions per unit time

$$m_{\text{CO}_2,v,\text{tot}} := \gamma \cdot \sum_{(i,j) \in \mathcal{A}_R} e_{ij} \cdot \left(f_0(i, j) + \sum_{m \in \mathcal{M}} f_m(i, j) \right), \quad (11)$$

where γ relates the energy consumption and the CO₂ emissions. We assume that customers trips and AMoD rebalancing strategies are chosen to maximize the customers welfare, defined through the average travel time t_{avg} . Hence, we link the functionality and resources of the I-AMoD DP through the following optimization problem:

$$\min_{\{f_m(\cdot, \cdot)\}_m, f_0(\cdot, \cdot)} t_{\text{avg}} = \frac{1}{\alpha_{\text{tot}}} \sum_{m \in \mathcal{M}, (i,j) \in \mathcal{A}} t_{ij} \cdot f_m(i, j) \quad \text{s.t. Eq. (1), Eq. (4), Eq. (6)}. \quad (12)$$

Formally, $\mathcal{F}_0 = \overline{\mathbb{R}}_+$, and $\mathcal{R}_0 = \overline{\mathbb{R}}_+ \times \mathbb{N} \times \mathbb{N} \times \overline{\mathbb{R}}_+ \times \overline{\mathbb{R}}_+ \times \overline{\mathbb{R}}_+$. Note that in general, the optimization problem (12) might possess multiple optimal solutions, making the relation between resources and functionality ill-posed. To overcome this subtlety, if two solutions share the same average travel time, we select the one incurring in the *lowest* mileage.

4.2.4. The Monotone Co-Design Problem

The full-system CDP results from the interconnection of the DPs presented above. A schematic representation is shown in Figure 2d. The functionality of the system is to provide mobility service to the customers, quantified, as in (8), by means of the total request rate. To this end, the following three resources are required. First, on the customers side, we require an average travel time, defined

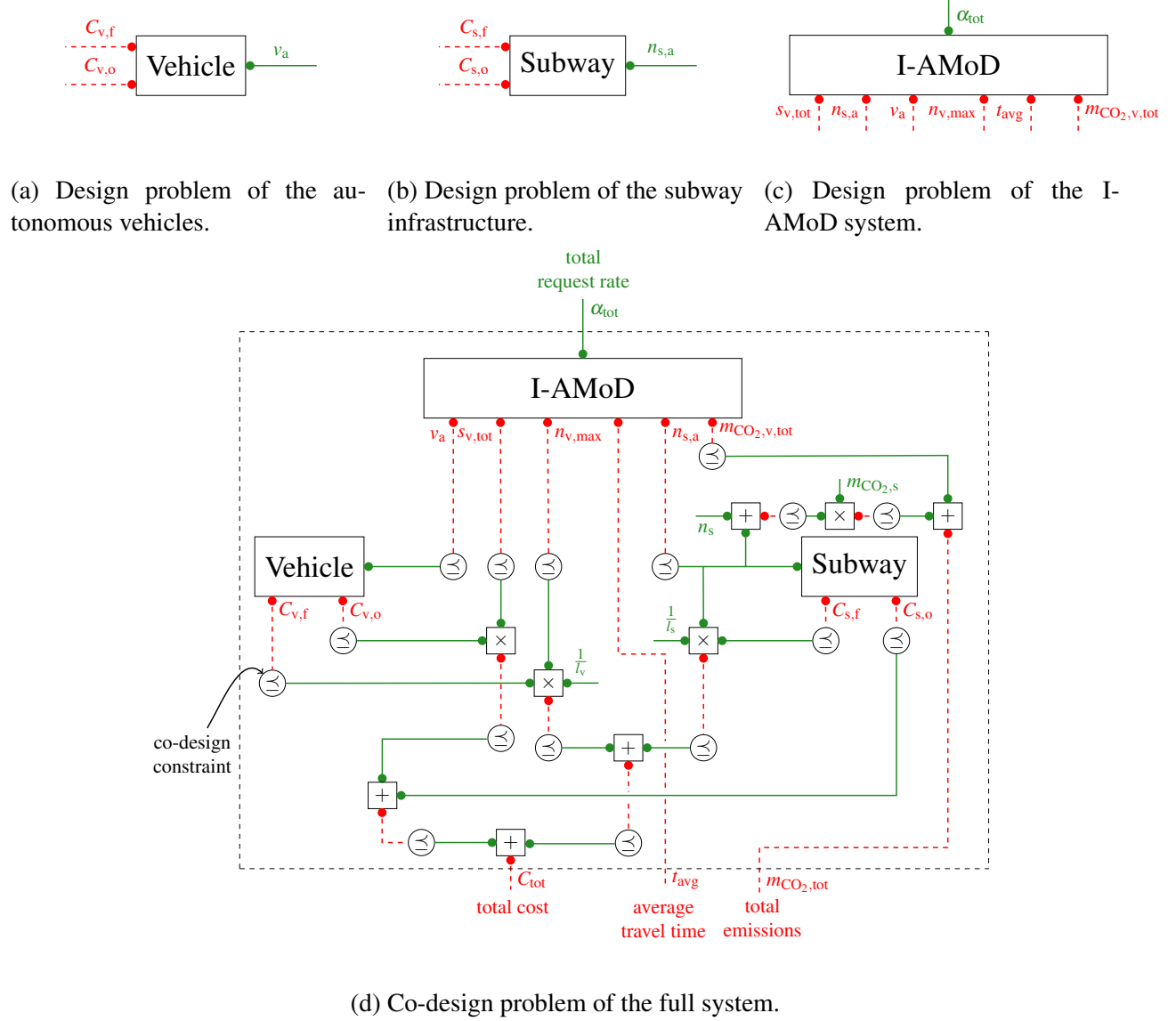


FIGURE 2: Schematic representation of the individual design problems (a-c) as well as of the co-design problem of the full system (d). In solid green the provided functionalities and in dashed red the required resources. The edges in the co-design diagram (d) represent co-design constraints: The resources required by a first design problem are the lower bound for the functionalities provided by the second one.

as in (9). Second, on the central authority side, the resource is the total transportation cost of the intermodal mobility system: Assuming an average vehicles' life of l_v , an average trains' life of l_s , and a baseline subway fleet of $n_{s,baseline}$ trains, we express the total costs as

$$C_{tot} = C_v + C_s, \quad (13)$$

where C_v is the AVs-related cost

$$C_v = \frac{C_{v,f}}{l_v} \cdot n_v + C_{v,o} \cdot s_{v,tot}, \quad (14)$$

and C_s is the public transit-related cost

$$C_s = \frac{C_{s,f}}{l_s} \cdot n_{s,a} + C_{s,o}. \quad (15)$$

Third, on the environmental side, the resources is the total CO₂ emissions

$$m_{CO_2,tot} = m_{CO_2,v,tot} + m_{CO_2,s} \cdot n_s, \quad (16)$$

where $m_{CO_2,s}$ represents the CO₂ emissions of a single train. Formally, α_{tot} is the CDP functionality, whereas t_{avg} , C_{tot} , and $m_{CO_2,tot}$ are the resources. Consistently, the functionality space is $\mathcal{F} = \overline{\mathbb{R}}_+$ and the resources space is $\mathcal{R} = \overline{\mathbb{R}}_+ \times \overline{\mathbb{R}}_+ \times \overline{\mathbb{R}}_+$. Note that the resulting CDP is indeed monotone, since it consists of the interconnection of monotone DPs [1].

4.3. Discussion

A few comments are in order. First, we lump the vehicle autonomy in its achievable velocity. We leave to future research more elaborated AV models, accounting for instance for accidents rates [26] and for safety levels. Second, we assume the service frequency of the subway system to scale linearly with the number of trains. We inherently rely on the assumption that the existing infrastructure can homogeneously accommodate the acquired train cars. To justify the assumption, we include an upper bound on the number of potentially acquirable trains in our case study design in Section 5. Third, we highlight that the I-AMoD framework is only one of the many feasible ways to map total demand to travel time, costs, and emissions. Specifically, practitioners can easily replace the corresponding DP with more sophisticated models (e.g., simulation-based frameworks like MATSim [27]), as long as the monotonicity of the system is preserved. In our setting, we conjecture the customers and vehicles routes to be centrally controlled by the central authority in a socially-optimal fashion. Fourth, we assume a homogenous fleet of AVs. Nevertheless, our model is readily extendable to capture heterogeneous fleets. Finally, we consider a fixed travel demand, and compute the antichain of resources providing it. Nonetheless, our formalization can be readily extended to arbitrary demand models preserving the monotonicity of the CDP (accounting for instance for elastic and stochastic effects). We leave this topic to future research.

5. Results

In this section, we leverage the framework presented in Section 4 to evaluate the real-world case of Washington D.C., USA. Section 5.1 details the case study. We then present numerical results in Sections 5.2 and 5.3.

5.1. Case Study

We present our studies on the real-world case of Washington D.C., USA. We import the road network (Figure 1b) and its features from OpenStreetMap [28]. The public transit network and its schedules are extracted from the GTFS data [29]. The travel demand is obtained by unifying the origin-destination pairs of the morning peak of May 31st 2017 provided by the taxi companies [30]

and the Washington Metropolitan Area Transit Authority (WMATA) [23]. Given the lack of reliable demand data for the MetroBus system, we focus our studies on the MetroRail system and its design, inherently assuming MetroBus commuters to be unaffected by our design methodology. To account for the large presence of ride-hailing companies, we scale the taxi demand rate by a factor of 5 [31]. Overall, the demand dataset includes 15,872 travel requests, corresponding to a demand rate of 24.22 requests/s. To account for congestion effects, we compute the nominal road capacity as in [32] and assume an average baseline road usage of 93%, in line with [33]. We summarize the main parameters together with their bibliographic sources in Table 1. In the remainder of this section, we tailor and solve the co-design problem presented in Section 4 through the PyMCDP solver [34], and investigate the influence of different AVs costs on the design objectives and strategies.

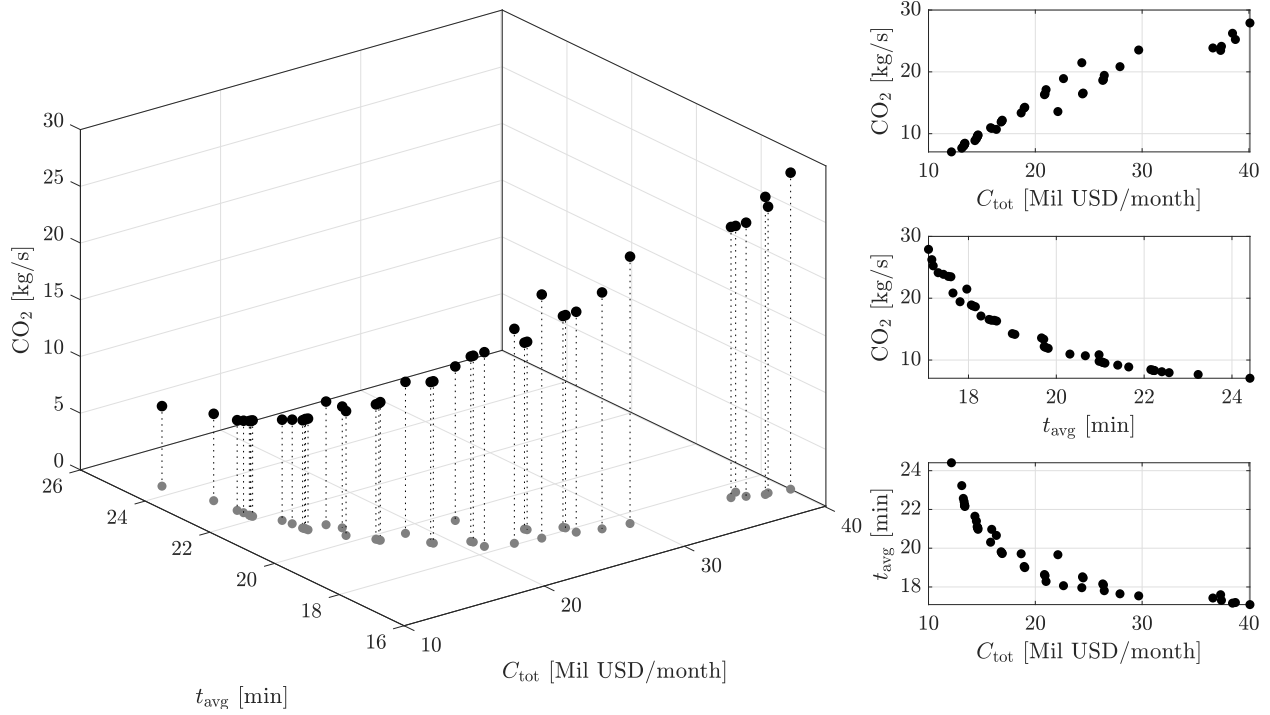
Parameter	Variable	Value					Units	Source
Baseline road usage	u_{ij}	93					%	[33]
		Case 1	Case 2.1	Case 2.2	Case 3.1	Case 3.2		
Vehicle operational cost	$C_{v,o}$	0.084	0.084	0.062	0.084	0.084	USD/mile	[35, 36]
Vehicle cost	$C_{v,v}$	32,000	32,000	26,000	32,000	32,000	USD/car	[35]
	20 mph	15,000	20,000	3,700	0	500,000	USD/car	[36–40]
	25 mph	15,000	30,000	4,400	0	500,000	USD/car	[36–40]
	30 mph	15,000	55,000	6,200	0	500,000	USD/car	[36–40]
Vehicle automation cost	$C_{v,a}$	15,000	90,000	8,700	0	500,000	USD/car	[36–40]
	35 mph	15,000	115,000	9,800	0	500,000	USD/car	[36–40]
	40 mph	15,000	130,000	12,000	0	500,000	USD/car	[36–40]
	45 mph	15,000	150,000	13,000	0	500,000	USD/car	[36–40]
Vehicle life	l_v	5	5	5	5	5	years	[35]
CO ₂ per Joule	γ	0.14	0.14	0.14	0.14	0.14	g/kJ	[41]
Time from \mathcal{G}_W to \mathcal{G}_R	t_{WR}	300	300	300	300	300	s	-
Time from \mathcal{G}_R to \mathcal{G}_W	t_{RW}	60	60	60	60	60	s	-
Speed limit fraction	β	$\frac{1}{1.3}$	$\frac{1}{1.3}$	$\frac{1}{1.3}$	$\frac{1}{1.3}$	$\frac{1}{1.3}$	-	[21]
	100 %	148,000,000					USD/year	[42]
Subway operational cost	133 %	197,000,000					USD/year	[42]
	200 %	295,000,000					USD/year	[42]
Subway fixed cost	$C_{s,f}$	14,500,000					USD/train	[43]
Train life	l_s	30					years	[43]
Subway CO ₂ emissions per train	$m_{CO_2,s}$	140					ton/year	[44]
Train fleet baseline	$n_{s,baseline}$	112					trains	[43]
Subway service frequency	$\phi_{j,baseline}$	$\frac{1}{6}$					1/minutes	[45]
Time from \mathcal{G}_W to \mathcal{G}_P and vice-versa	t_{WS}	60					s	-

TABLE 1: Parameters, variables, numbers, and units for the case studies.

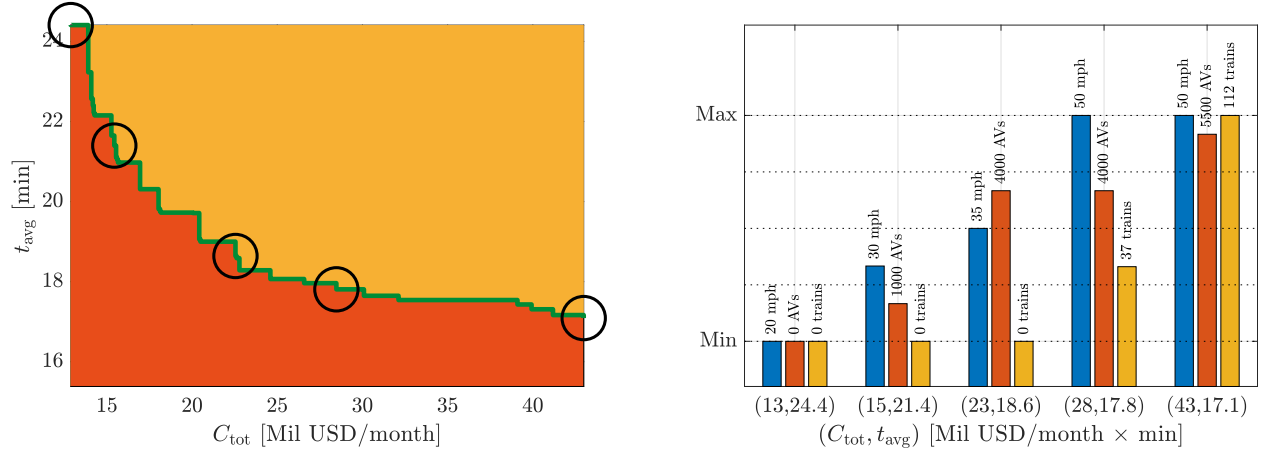
5.2. Case 1 - Constant Cost of Automation

In line with [36–40], we first assume an average achievable-velocity-independent cost of automation. As discussed in Section 4, we design the system by means of subway service frequency, AVs fleet size, and achievable free-flow speed. Specifically, we allow the municipality to (i) increase the subway service frequency ϕ_j by a factor of 0%, 33%, or 100%, (ii) deploy an AMoD fleet of size $n_{v,max} \in \{0, 500, 1000, \dots, 6000\}$ vehicles, and (iii) design the single AV achievable velocity $v_a \in \{20 \text{ mph}, 25 \text{ mph}, \dots, 50 \text{ mph}\}$. We assume the AMoD fleet to be composed of battery electric BEV-250 mile vehicles [35]. In Figure 3a, we show the solution of the co-design problem by reporting the antichain consisting of the total transportation cost, average travel time, and total CO₂ emissions. These solutions are *rational* (and not comparable) in the sense that there exists

no instance which simultaneously yields lower cost, average travel time, and emissions. For the



(a) Tri-dimensional representation antichain elements and their projection in the cost-time space (left) and their two-dimensional projections (right).



(b) Results for asymptotic automation costs. On the left, the two-dimensional representation of the antichain elements: in red are the unfeasible strategies, in orange the feasible but irrational solutions, and in green the Pareto front. On the right, the implementations corresponding to the highlighted antichain elements, quantified in terms of achievable vehicle speed, AVs fleet size, and train fleet size.

FIGURE 3: Solution of the Co-Design Problem (CDP) for the state-of-the art case.

sake of clarity, we opt for a two-dimensional antichain representation, by translating and includ-

ing the emissions in the total cost. To do so, we consider the conversion factor 40 USD/kg [46]. Note that since this transformation preserves the monotonicity of the CDP it smoothly integrates in our framework. Doing so, we can conveniently depict the co-design strategies through the two-dimensional antichain (Figure 3b, right) and the corresponding municipality actions (Figure 3b, left). Generally, as the municipality budget increases, the average travel time per trip required to satisfy the given demand decreases, reaching a minimum of about 17.1 minutes with a monthly expense of around $43,000,000 \text{ USD/month}$. This configuration corresponds to a fleet 5,500 AVs able to drive at 50 mph and to the doubling of the current MetroRail train fleet. On the other hand, the smallest rational investment of $12,900,000 \text{ USD/month}$ leads to a 42 % higher average travel time, corresponding to a non-existent autonomous fleet and an unchanged subway infrastructure. Notably, an expense of $23,000,000 \text{ USD/month}$ (48 % lower than the highest rational investment) only increases the minimal required travel time by 9 %, requiring a fleet of 4,000 vehicles able to drive at 35 mph and no acquisition of trains. Conversely, an investment of $15,600,000 \text{ USD/month}$ (just $2,700,000 \text{ USD/month}$ more than the minimal rational investment) provides a 3 min shorter travel time. Remarkably, the design of AVs able to exceed 40 mph only improves the average travel time by 6 %, and it is rational just starting from an expense of $22,800,000 \text{ USD/month}$. This suggests that the design of faster vehicles mainly results in higher emission rates and costs, without substantially contributing to a more time-efficient demand satisfaction. Finally, it is rational to improve the subway system only starting from a budget $28,500,000 \text{ USD/month}$, leading to a travel time improvement of just 4 %. This trend can be explained with the high train acquisition and increased operation costs, related to the subway reinforcement. We expect this phenomenon to be more marked for other cities, considering the moderate operation costs of the MetroRail subway system due to its automation [45] and related benefits [47].

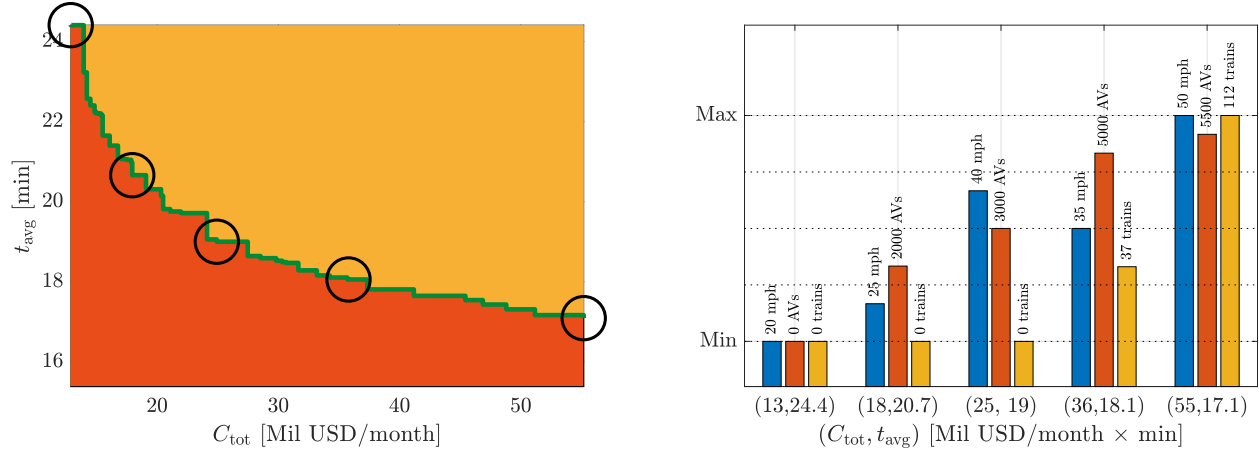
5.3. Case 2 - Speed-Dependent Automation Costs

To relax the potentially unrealistic assumption of a velocity-independent automation cost, we consider a performance-dependent cost structure. The large variance in sensing technologies and their reported performances [48] suggests that this rationale is reasonable. Indeed, the technology required today to safely operate an autonomous vehicle at 50 mph is substantially more sophisticated, and therefore more expensive, than the one needed at 20 mph. To this end, we adopt the cost structure reported in Table 1. Furthermore, the frenetic evolution of automation techniques intricates their monetary quantification [49]. Therefore, we perform our studies with current (2019) costs as well as with their projections for the upcoming decade (2025) [35, 50].

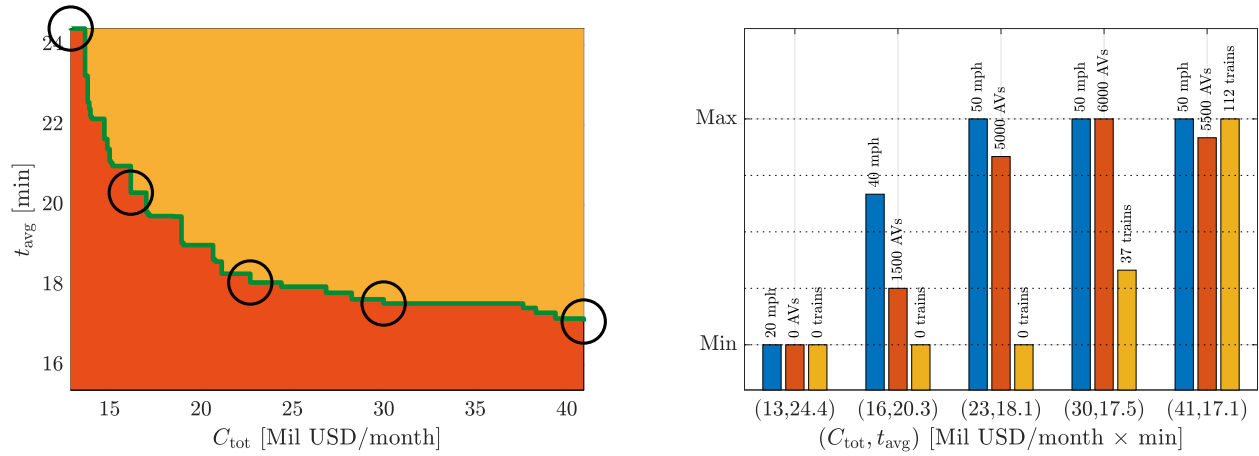
5.3.1. Case 2.1 - 2019

Here, we study the hypothetical case of an immediate AVs fleet deployment, assuming the technological advances to be provided. We introduce the aforementioned velocity-dependent automation cost structure and obtain the results reported in Figure 4a. Comparing these results with the state-of-the-art values presented in Figure 3 confirms the previously observed trend concerning elevated vehicle speeds. Indeed, spending $24,900,000 \text{ USD/month}$ (55 % lower than the highest rational expense) only increases the average travel time by 10 %, requiring a fleet of 3,000 AVs at 40 mph and no subway interventions. Nevertheless, the comparison shows two substantial differences. First, the budget required to reach the minimum travel time of 17.1 minutes is 28 % higher compared to the previous case, and consists of the same strategy for the municipality, i.e., doubling the train fleet and having a fleet of 5,500 AVs at 50 mph. Second, the higher vehicle costs result in an av-

average AVs fleet growth of 5 %, an average velocity reduction of 9 %, and an average train fleet growth of 7 %. The latter suggests a shift towards a poorer AVs performance in favour of fleets enlargements.



(a) Speed-dependent automation costs in 2019.



(b) Speed-dependent automation costs in 2025.

FIGURE 4: Results for the speed-dependent automation costs. On the left, the two-dimensional representation of the antichain elements: in red are the unfeasible strategies, in orange the feasible but irrational solutions, and in green the Pareto front. On the right, the implementations corresponding to the highlighted antichain elements.

5.3.2. Case 2.2 - 2025

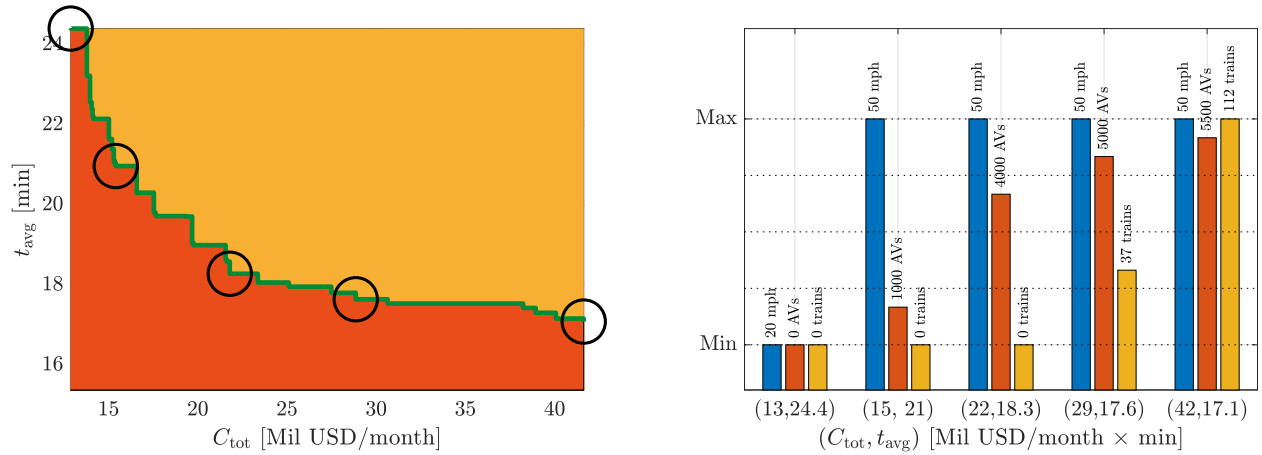
Experts forecast a large automation cost reduction (up to 90 %) in the next decade, due to mass-production of the AVs sensing technology [49, 50]. In line with this vision, we inspect the futuristic scenario by solving the co-design problem for the adapted automation costs, and report the results in Figure 4b. Two comments are in order. First, one can notice that the maximal rational budget is 25 % lower than in the immediate adoption case. Second, the reduction in autonomy costs clearly eases the acquisition of more performant AVs, increasing the average vehicle speed by 10 %. As a direct consequence, the AVs and train fleets are reduced in size by 5 % and 10 %, respectively.

5.4. Case 3 - Asymptotic Automation Cost Analysis

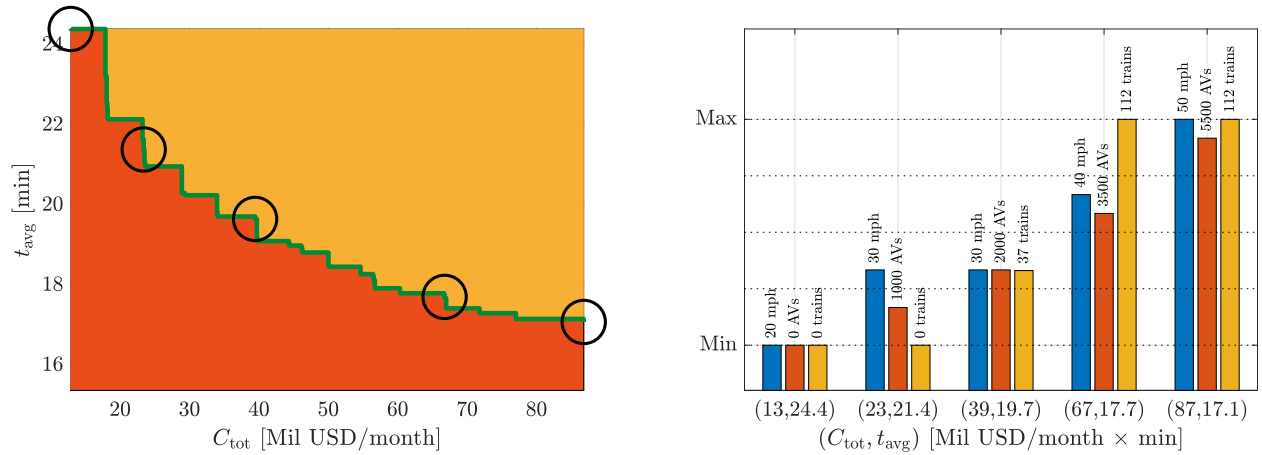
We conclude our numerical analysis with a study on asymptotic cost structures. Specifically, we compare the constrasting cases of a free-of-charge and a very high (500,000 USD/car) automation cost.

5.4.1. Case 3.1- No Automation Cost

This case could represent the future full deployment of AVs, where the cost of automation is naturally included in the normal production costs and does not represent an additional expense. The results for this cost structure are reported in Figure 5a. Notably, the Pareto front is very similar to the one presented in Figure 3, leading to just a 5 % increase in the AVs speed and to invariate fleet sizes. Clearly, the assumption a cost-free automation favours the deployment of AVs at the expenses of subway improvements.



(a) Results for no automation costs.



(b) Results for large automation costs.

FIGURE 5: Results for asymptotic automation costs. On the left, the two-dimensional representation of the antichain elements: in red are the unfeasible strategies, in orange the feasible but irrational solutions, and in green the Pareto front. On the right, the implementations corresponding to the highlighted antichain elements.

5.4.2. Case 3.2- High Automation Cost

In this case we assume a performance-independent automation cost of 500,000 USD/car. Although this cost may appear unreasonably large, it roughly captures the extremely onerous research and development costs which AVs companies are facing today [51]. Indeed, no company has shown the ability to safely and reliably deploy large fleets of AVs yet. The results, reported in Figure 5b, show different trends from the ones depicted in Figure 5a. First, we observe substantial shift towards an increase of 163 % in the average train fleet size, followed by a 17 % decrease in the average AVs fleet size. Second, to reach the minimal rational average travel time, one needs an expense of roughly 87,000,000 USD/month, corresponding to a 107 % higher investment.

5.5. Discussion

A few comments are in order. First, the presented case studies illustrate the ability of our framework to extract the set of rational design strategies for an AVs-enabled mobility system. This way, stakeholders such as AVs companies, transportation authorities, and policy makers get transparent and interpretable insights on the impact of future interventions. Second, we perform a sensitivity analysis (Figure 6) through the variation of the autonomy cost structures. On the one hand, this reveals a clear transition from small fleets of fast AVs (in the case of low autonomy costs) to a fleet of numerous slow vehicles (in the case of high autonomy costs). On the other hand, our studies highlight that investments in the public transit infrastructure are rational only when large budgets are available. Indeed, the onerous train acquisition and operation costs lead to a comparative advantage of AVs-based mobility. In the future, we plan to collect more high-resolution data to corroborate our conclusions with quantitative results.

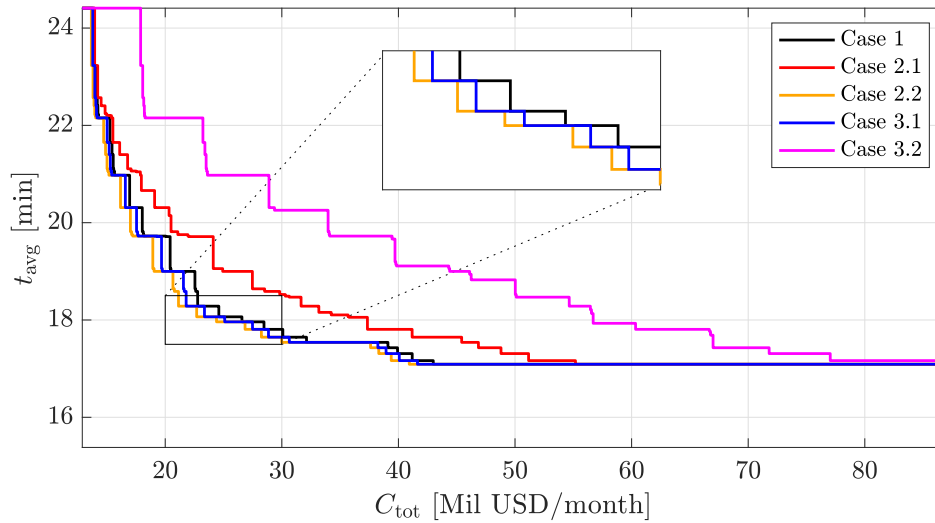


FIGURE 6: Comparison of the antichains resulting from different case studies.

6. Conclusion

In this paper, we leveraged the mathematical theory of co-design to propose a design framework for AVs-enabled mobility systems. Specifically, the nature of our framework allows both for the modular and compositional interconnection of the design problems of different mobility options

and for multiple objectives. Starting from the multi-commodity flow model of an intermodal autonomous mobility-on-demand system, we designed autonomous vehicles and public transit both from a vehicle-centric and fleet-level perspective. In particular, we studied the problem of deploying a fleet of self-driving vehicles providing on-demand mobility in cooperation with public transit, adapting the speed achievable by the vehicles, the fleet size, and the service frequency of the subway lines. Our framework allows the stakeholders involved in the mobility ecosystem, from vehicle developers all the way to mobility-as-a-service companies and governmental authorities, to characterize rational trajectories for technology and investment development. We showcased our methodology on the real-world case study of Washington D.C., USA. Notably, we showed how our problem formulation allows for a systematic analysis of incomparable objectives, providing stakeholders with analytical insights for the socio-technical design of AVs-enabled mobility systems. This work opens the field for the following future research streams:

Modeling: First, we would like to extend the presented framework to capture additional modes of transportation, such as buses, bikes, and e-scooters, and heterogeneous fleets with different self-driving infrastructures, propulsion systems, and passenger capacity. Second, we would like to include the possibility of accommodating the design of public transit lines. Third, we would like to investigate variable demand models. Finally, we would like to analyze the interactions between multiple stakeholders, characterizing the equilibrium arising from their conflicting interests.

Algorithms: It is of interest to tailor general co-design algorithmic frameworks to the particular case of transportation design problems, possibly leveraging their specific structure.

Application: Finally, we would like to devise a web interface which supports mobility stakeholders to reason on strategic interventions in urban areas.

7. Acknowledgements

We would like to thank Dr. Riccardo Bonalli, Dr. Maximilian Schiffer, Matthew Tsao, Dr. Kaidi Yang, and Dr. Stephen Zoepf for the fruitful discussions, Ms. Sonia Monti for the I-AMoD illustration, and Dr. Ilse New for proofreading the manuscript. The first author would like to thank the Traugott and Josefine Niederberger-Kobold Foundation and FISITA for their financial support. The second author would like to thank the Zeno-Karl Schindler Foundation for the financial support. This research was supported by the National Science Foundation under CAREER Award CMMI-1454737 and the Toyota Research Institute (TRI). This article solely reflects the opinions and conclusions of its authors and not NSF, TRI, or any other entity.

8. Statement of Contributions

The authors confirm contribution to the paper as follows: study conception and design: Gioele Zardini, Nicolas Lanzetti, Mauro Salazar, Andrea Censi, and Marco Pavone, data collection: Gioele Zardini, Nicolas Lanzetti, analysis and interpretation of results: Gioele Zardini, Nicolas Lanzetti, Mauro Salazar, Andrea Censi, and Marco Pavone, draft manuscript preparation: Gioele Zardini, Nicolas Lanzetti, Mauro Salazar, Andrea Censi, Emilio Frazzoli, and Marco Pavone.

All authors reviewed the results and approved the final version of the manuscript.

9. References

1. Censi, A., A Mathematical Theory of Co-Design. *arXiv preprint arXiv:1512.08055v7*, 2015.
2. Censi, A., Monotone Co-Design Problems; or, everything is the same. In *American Control Conference*, 2016.
3. Censi, A., A Class of Co-Design Problems With Cyclic Constraints and Their Solution. *IEEE Robotics and Automation Letters*, Vol. 2, 2017, pp. 96–103.
4. Salazar, M., N. Lanzetti, F. Rossi, M. Schiffer, and M. Pavone, Intermodal Autonomous Mobility-on-Demand. *IEEE Transactions on Intelligent Transportation Systems*, 2019, in press.
5. Farahani, R. Z., E. Miandoabchi, W. Y. Szeto, and H. Rashidi, A review of urban transportation network design problems. *European Journal of Operational Research*, Vol. 229, 2013, pp. 281–302.
6. Wang, D. Z. W. and H. K. Lo, Global Optimum of the Linearized Network Design Problem with Equilibrium Flows. *Transportation Research Part B: Methodological*, Vol. 44, No. 4, 2010, pp. 482–492.
7. Cong, Z., B. De Schutter, and R. Babuska, Co-design of traffic network topology and control measures. *Transportation Research Part C: Emerging Technologies*, Vol. 54, 2015, pp. 56–73.
8. Guihaire, V. and J.-K. Hao, Transit network design and scheduling: A global review. *Transportation Research Part B: Methodological*, Vol. 42, 2008, pp. 1251–1273.
9. Cipriani, E., S. Gori, and M. Petrelli, Transit network design: a procedure and an application to a large urban area. *Transportation Research Part C: Emerging Technologies*, Vol. 20, No. 1, 2012, pp. 2–14.
10. Miandoabchi, E., R. Z. Farahani, and W. Y. Szeto, Bi-objective bimodal urban road network design using hybrid metaheuristics. *Central European Journal of Operational Research*, Vol. 20, No. 4, 2012, pp. 583–621.
11. Barrios, J. A. and J. C. Doig, Fleet sizing for flexible carsharing systems: a simulation-based approach. In *Annual Meeting of the Transportation Research Board*, 2013.
12. Barrios, J. A. and J. D. Godier, Fleet Sizing for Flexible Carsharing Systems: Simulation-Based Approach. *Transportation Research Record: Journal of the Transportation Research Board*, Vol. 2416, 2014, pp. 1–9.
13. Fagnant, D. J. and K. M. Kockelman, Dynamic ride-sharing and fleet sizing for a system of shared autonomous vehicles in Austin, Texas. *Transportation*, Vol. 45, No. 1, 2018, pp. 143–158.
14. Spieser, K., K. Treleaven, R. Zhang, E. Frazzoli, D. Morton, and M. Pavone, Toward a Systematic Approach to the Design and Evaluation of Autonomous Mobility-on-Demand Systems: A Case Study in Singapore. In *Road Vehicle Automation*, Springer, 2014.
15. Zhang, H., C. J. R. Sheppard, T. Lipman, and M. S. J., Joint Fleet Sizing and Charging System Planning for Autonomous Electric Vehicles. *arXiv preprint arXiv:1811.00234*, 2018.
16. Beaujon, G. J. and M. A. Turnquist, A Model for Fleet Sizing and Vehicle Allocation. *Transportation Science*, Vol. 25, No. 1, 1991, pp. 19–45.
17. Liu, Y., P. Bansal, R. Daziano, and S. Samaranayake, A framework to integrate mode choice in the design of mobility-on-demand systems. *Transportation Research Part C*:

- Emerging Technologies*, 2018, in press. Available online at <https://doi.org/10.1016/j.trc.2018.09.022>.
18. Sayarshad, H. R. and R. Tavakkoli-Moghaddam, Solving a multi periodic stochastic model of the rail-car fleet sizing by two-stage optimization formulation. Vol. 34, 2010, pp. 1164–1174.
 19. Pinto, H. K. R. F., M. F. Hyland, H. S. Mahmassani, and I. O. Verbas, Joint design of multimodal transit networks and shared autonomous mobility fleets. *Transportation Research Part C: Emerging Technologies*, 2019, in press. Available online at <https://doi.org/10.1016/j.trc.2019.06.010>.
 20. Davey, B. A. and H. A. Priestley, *Introduction to Lattices and Order*. Cambridge University Press, second edition ed., 2002.
 21. Dahl, D., *If you're annoyed at drivers going under the speed limit, the problem isn't them, it's you*. The Bellingham Herald, 2018, available online.
 22. Daganzo, C. F. and N. Geroliminis, An analytical approximation for the macroscopic fundamental diagram of urban traffic. *Transportation Research Part B: Methodological*, Vol. 42, No. 9, 2008, pp. 771–781.
 23. PIM, *Metrorail Ridership by Origin and Destination*. Plan It Metrot, 2012, available online at <https://planitmetro.com/2012/10/31/data-download-metrorail-ridership-by-origin-and-destination/>.
 24. Salazar, M., F. Rossi, M. Schiffer, C. H. Onder, and M. Pavone, On the Interaction between Autonomous Mobility-on-Demand and the Public Transportation Systems. In *Proc. IEEE Int. Conf. on Intelligent Transportation Systems*, 2018, Extended Version, Available at <https://arxiv.org/abs/1804.11278>.
 25. Mas-Colell, A., M. D. Whinston, and J. R. Green, *Microeconomic Theory*. Oxford Univ. Press, 1995.
 26. Richards, D. C., *Relationship between Speed and Risk of Fatal Injury: Pedestrians and Car Occupants*. Department for Transport: London, 2010.
 27. Horni, A., K. Nagel, and K. W. Axhausen (eds.) *The Multi-Agent Transport Simulation MATSim*. Ubiquity Press, 2016.
 28. Haklay, M. and P. Weber, OpenStreetMap: User-Generated Street Maps. *IEEE Pervasive Computing*, Vol. 7, No. 4, 2008, pp. 12–18.
 29. GTFS, *GTFS: Making Public Transit Data Universally Accessible*, 2019, available online at <https://gtfs.org/>.
 30. ODDC, *Taxicab Trips in 2016*. Open Data DC, 2017, available online at <https://opendata.dc.gov/search?q=taxicabs>.
 31. Siddiqui, F., *As ride hailing booms in D.C., it's not just eating in the taxi market – it's increasing vehicle trips*. The Washington Post, 2018, available online.
 32. DoA (ed.) *Military Police Traffic Operations*. Department of the Army, 1977.
 33. Dixon, S., H. Irshad, and V. White, *Deloitte City Mobility Index – Washington D.C.*. Deloitte, 2018.
 34. Censi, A., *Monotone Co-Design Problems*, 2019, available online: <https://co-design.science/index.html>.
 35. Pavlenko, N., P. Slowik, and N. Lutsey, *When does electrifying shared mobility make economic sense?* The International Council on Clean Transportation, 2019.

36. Boesch, P. M., F. Becker, H. Becker, and K. W. Axhausen, Cost-based analysis of autonomous mobility services. *Transport Policy*, Vol. 64, 2018, pp. 76–91.
37. Fagnant, D. J. and K. Kockelman, Preparing a nation for autonomous vehicles: opportunities, barriers and policy recommendations. *Transportation Research Part A: Policy and Practice*, Vol. 77, 2015, pp. 167–181.
38. Bauer, G. S., J. B. Greenblatt, and B. F. Gerke, Cost, Energy, and Environmental Impact of Automated Electric Taxi Fleets in Manhattan. *Environmental Science & Technology*, Vol. 52, No. 8, 2018, pp. 4920–4928.
39. Litman, T., *Autonomous Vehicle Implementation Predictions – Implications for Transport Planning*. Victoria Transport Policy Institute, 2019.
40. Wadud, Z., Fully automated vehicles: A cost of ownership analysis to inform early adoption. *Transportation Research Part A: Policy and Practice*, Vol. 101, 2017, pp. 163–176.
41. Time, W., *Carboon Footprint Data*, 2018, Available at <https://api.watvertime.org>. Retrieved on March 23, 2018.
42. WMATA, *FY2018 Proposed Budget*. Washington Metropolitan Area Transit Authority, 2017.
43. Aratani, L., *Metro to debut first of its 7000-series cars on Blue Line on April 14*. The Washington Post, 2015, available online.
44. WMATA, *Sustainability Report 2018*. Washington Metropolitan Area Transit Authority, 2018.
45. Jaffe, E., *The Case for Driverless Trains, By the Numbers*. Citylab, 2015, available online.
46. Howard, P. and D. Sylvan, *Expert Consensus on the Economics of Climate Change*. Institute for Policy Integrity – New York University School of Law, 2015.
47. Wang, Y., J. Zhang, M. Ma, and X. Zhou, Survey on Driverless Train Operation for Urban Rail Transit Systems. Vol. 2, No. 3–4, 2016, pp. 106—113.
48. Gawron, J. H., G. A. Keoleian, R. D. De Kleine, T. J. Wallington, and K. Hyung Chul, Life Cycle Assessment of Connected and Automated Vehicles: Sensing and Computing Subsystem and Vehicle Level Effects. *Environmental Science & Technology*, Vol. 52, 2018, pp. 3249–3256.
49. WCP, *The Automotive LiDAR Market*. Woodside Capital Partners, 2018.
50. Lienert, P., *Cost of Driverless Vehicles to Drop Dramatically: Delphi CEO*. Insurance Journal, 2019, available online.
51. Korosec, K., *Uber spent USD 457 million on self-driving and flying car R&D last year*. TechCrunch, 2019, available online.